Effect of Zn^{2+} and K^+ as Retarding Agents on Rock-Based Geopolymers for Downhole Cementing Operations

Fawzi Chamssine[1]
Department of Energy and Petroleum Engineering,
Faculty of Science & Technology,
University of Stavanger,
4036 Stavanger, Norway
e-mail: fawzi.chamssine@uis.no

Mahmoud Khalifeh
Department of Energy and Petroleum Engineering,
Faculty of Science & Technology,
University of Stavanger,
4036 Stavanger, Norway
e-mail: mahmoud.khalifeh@uis.no

Arild Saasen
Department of Energy and Petroleum Engineering,
Faculty of Science & Technology,
University of Stavanger,
4036 Stavanger, Norway
e-mail: arild.saasen@uis.no

Geopolymer material has a potential to function alongside Portland Cement as an efficient cementitious material for well cementing and plug and abandonment applications. Geopolymer material requires retarding agents to be displaced into the well while considering the properties required to maintain efficient zonal isolation through superior mechanical properties. Chemical admixtures affect the material structure and can, in some cases, jeopardize material integrity if not engineered properly to suite downhole conditions. The present article shows the effect of Zn^{2+} and K^+ species have as retarding agents on slurry, mechanical, and microstructural properties. The approach has been carried out to obtain a preliminary overview of how retarding agents can behave in mix design slurries where eventually sealing performance was examined. Samples were cured and examined for periods of 1, 3, 7, 14, and 28 days at downhole conditions. The results obtained confirm a retardation effect by the addition of Zn^{2+} and K^+ species and some shortcomings in early strength development due to a poisoning mechanism by Zn^{2+} species. This phenomenon indicates the formation of Ca-Zn phase that can hinder the nucleation of the geopolymeric gel structure. No significant effects were observed on the microstructural development throughout the curing period. The effect of Zn^{2+} species was also observed in increasing threshold for hydraulic sealability. It may be concluded that the tested retarding agents require furthermore development to minimize shortcomings in mechanical properties specifically early strength development. [DOI: 10.1115/1.4053710]

Keywords: geopolymers, zinc retarder, workability, strength development, sealability, petroleum engineering, petroleum wells-drilling/production/construction

1 Introduction

Alternative materials to Ordinary Portland Cement (OPC) have been studied throughout the past decades motivated by improving performance properties, lower cost, and lower environmental impact through the reduction in emission of greenhouse gases (e.g., CO_2, NO_x) [1]. One of the suggested materials is an alternative to OPC known as geopolymers [2–4]. These materials were first introduced by Joseph Davidovits in the 1970s as a material with potential properties to replace OPC [5–10]. Multiple studies presented some plausible shortcomings of OPC, which are related to the short- and long-term performance of OPC at operational conditions [11–19]. Thus, geopolymers have attracted the petroleum industry specifically due to the lower environmental impact during production, outstanding short- and long-term performance, and lower production cost by lowering taxable carbon emissions [20,21]. To create a lateral comparison, it is important to test geopolymer slurries at real field conditions to observe the closest effect of these conditions while testing on a lab-scale. The use of retarding agents is vital to make this material pumpable in cementing operations. Elevated downhole temperatures contribute in higher activation energy levels to geopolymer material, but at the same time limit material's applications specifically in well cementing operations [22]. Previous studies exhibited the effect of Zn^{2+} in retarding chemical reactions in geopolymer systems [23,24], thus workability of material can be increased to achieve sufficient time for displacement from surface to target downhole area. On the other hand, K^+ was utilized as a delayed accelerator to guaranty material setting and boost mechanical properties by allowing a controlled gelation reaction [25,26].

In the present study, zinc (Zn) and potassium (K) Nitrate have been used as chemical admixtures to adjust the slurry properties to prolong pumpability of the rock-based geopolymer for intermediate cementing operations. To address the objective of this study, two mix designs, a neat recipe, and a retarded recipe, were investigated under bottomhole circulating and static temperature and elevated pressure. The geopolymer material was prepared for downhole cementing operations in accordance with the set of tests presented in Fig. 1. Hydraulic sealability was conducted at the end to guaranty that material's integrity is not compromised due to the influence of retarding agents.

2 Materials and Methods

2.1 Materials and Mixing Procedure. The solid precursor used in this study was an aluminosilicate rich rock powder primarily made of granite, normalized with other precursors having reactive properties. The precursor was designed to have a low calcium content (<10 wt%). The solid precursor's composition is presented in Table 1. Potassium silicate solution with a modular ratio of 2.21 was used as the activating hardener phase. Distilled water was used to adjust total water content, viscosity of the slurries, and as a medium to introduce the chemical admixtures. Zinc nitrate hexahydrate ($N_2O_6Zn.6H_2O$) and potassium nitrate (KNO_3) were used, both with a purity of 99%. The amount of added chemical admixtures was adjusted to have a K^+/Zn^{2+} ratio of 0.25. The mix design of the neat sample (Geo-Neat) and retarded sample (Geo-Zn/K) is presented in Table 2. The used ratio was

[1]Corresponding author.

Contributed by the Petroleum Division of ASME for publication in the JOURNAL OF ENERGY RESOURCES TECHNOLOGY. Manuscript received October 25, 2021; final manuscript received January 24, 2022; published online February 21, 2022. Assoc. Editor: Yan Jin.

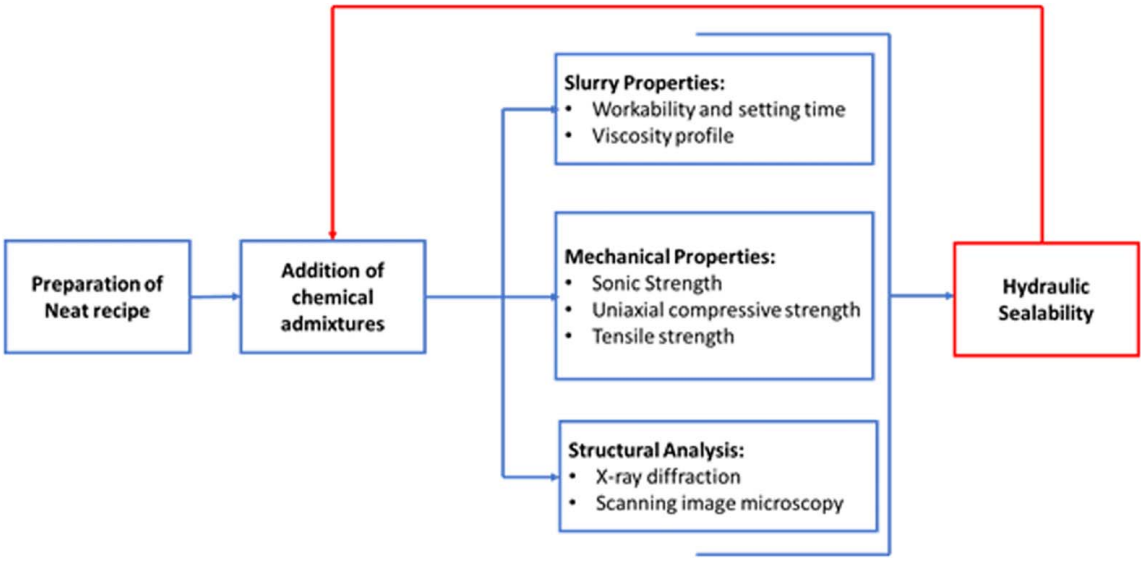

Fig. 1 Applied strategy for testing chemical admixtures in cementitious material slurries on a laboratory scale

experimentally concluded after running several tests and past experiences using the combination of both Zn^{2+} and K^{+} species [27].

The slurries were prepared with a solid to liquid ratio of 2.07. The mixing was carried out using a Waring high-speed blender with an OFITE control pad following the API RP 10B-2 recommendations [28].

2.1.1 Conditioning. Prior to some tests, conditioning of mix designs was conducted using an OFITE atmospheric consistometer (Model 60) following API RP 10B-2 recommendations [28]. Conditioning was performed at bottomhole circulating temperature (BHCT) of 50 °C and 150 rounds per minute (rpm), for a period of 30 min after reaching the desired BHCT. The purpose behind this process is to match the circulating slurry conditions and prepare it to match the static curing conditions to avoid any thermal shock to the slurry.

2.2 Slurry Properties

2.2.1 Workability and Setting Time. An OFITE HPHT consistometer (Model 2040) was used to examine the workability and setting time at a BHCT of 50 °C and pressure of 14 MPa. The temperature was ramped up at a rate of 1 °C/min and the pressure was ramped up from atmospheric to 14 MPa in a period of 10 min. The standard for workability was set from the starting point until 40 BC while setting time was from 40 BC to 100 BC following API RP 10-B2 recommendations [28].

2.2.2 Viscosity Measurements. Viscosity was measured using an OFITE Model 900 viscometer while tested at a BHCT of 50 °C. Ideally, these measurements should have been performed under pressure. To fulfill standard requirements, a large annular gap was necessary. Hence, the option was to use an atmospheric viscometer (OFITE Model 900 Rotational Viscometer). Addition of pressure would generally increase the viscosity slightly as the liquid phase is compressed and the efficient solid's fraction is slightly increased. The slurries were conditioned prior to testing.

Table 1 Solid phase composition

Chemical element	wt%
SiO_2	63.10
Al_2O_3	12.97
Fe_2O_3	1.49
CaO	9.94
MgO	4.54
Na_2O	2.34
K_2O	3.81
TiO_2	0.80
MnO	0.19
LOI	0.80
Total	100

2.3 Mechanical Properties

2.3.1 Sonic Strength. An OFITE Model 4005 automated twin cell ultrasonic cement analyzer (UCA) was used to examine the early strength development of the slurries. A sonic signal is emitted through the sample where the transit time of the signal is recorded [16]. Upon phase changes and setting, the velocity of transit time (time for sound to travel through the slurry) is increased. A correlation was used to convert the transit time recordings to sonic compressive strength. Since the default correlation is based on OPC parameters, a specific correlation was developed for geopolymer material using the results from the uniaxial compressive strength tests. The strength development was measured continuously for a period of 28 days at bottomhole static temperature (BHST) of 70 °C and pressure of 14 MPa.

Table 2 Mix design of tested slurries

	Sample composition (wt%)					
Mix design	Solid	Liquid	Total water	K^{+}	Zn^{2+}	K^{+}/Zn^{2+} ratio
GEO-Neat	66.23	53.77	22.13	–	–	–
GEO-Zn/K	66.23	53.77	22.13	0.075	0.3	0.25

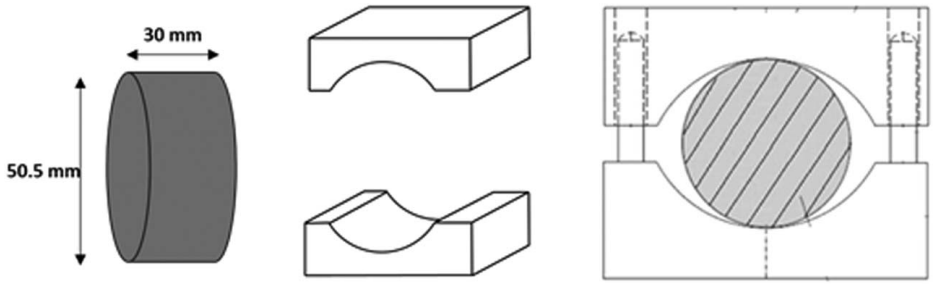

Fig. 2 Indirect tensile strength setup

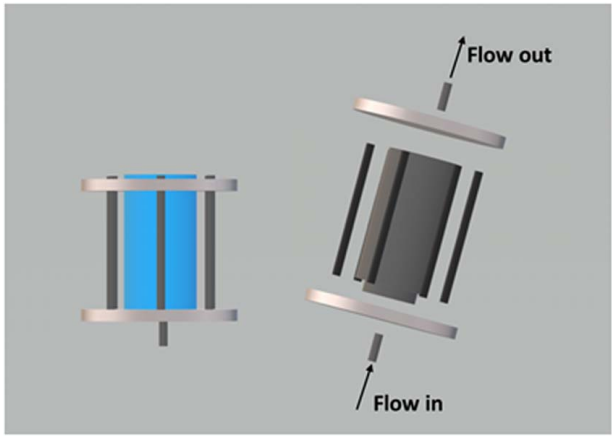

Fig. 3 Hydraulic sealability setup

2.3.2 Uniaxial Compressive Strength. The uniaxial compressive strength (UCS) tests were conducted using a Toni Technik-H mechanical tester in accordance with API TR 10TR7:2017 [29]. Cylindrical plastic molds of 50 mm diameter and 10 mm length were filled with slurries and positioned in cylindrical pressurized autoclaves filled with water where later a pressure buildup was applied using a Teledyne ISCO pump (Model 260D). Samples were cured at BHST of 70 °C and pressure of 14 MPa. The loading rate was selected to be 30 kN/min set at a force-controlled mode. Per curing period, three samples were tested, and the average compressive strength was calculated. The slurries were conditioned prior to curing.

2.3.3 Indirect Tensile Test (Brazilian Test). A Zwick/Roell Z050 material testing equipment was used to examine the tensile strength. Samples were cured at BHST of 70 °C and pressure of 14 MPa. Cured samples were cut in a disc-like shape having a thickness of 30 mm approximately. For each curing interval, four samples were prepared and tested to minimize any possible measurement error where the average tensile strength was calculated. The samples were later placed vertically in the setup described in Fig. 2. The compression load was 50 N/sec where the results were used to calculate the tensile strength based on Eq. (1) [30]. The average of the tested four samples was calculated and presented in the results. The slurries were conditioned prior to curing

$$\text{Tensile strength} = 1.2\,\frac{F}{\pi dl} \tag{1}$$

2.3.4 Hydraulic Sealability. To understand impact of the used admixtures on sealability (the objective using zonal isolation materials) of the final product, hydraulic integrity test was concluded. A cylindrical steel tube (KF HUP S355J2H) with diameter 82 mm and height of 150 mm and roughness of 1 μm of Ra was used to measure hydraulic sealability. The tube had a 2 side caps tightened with

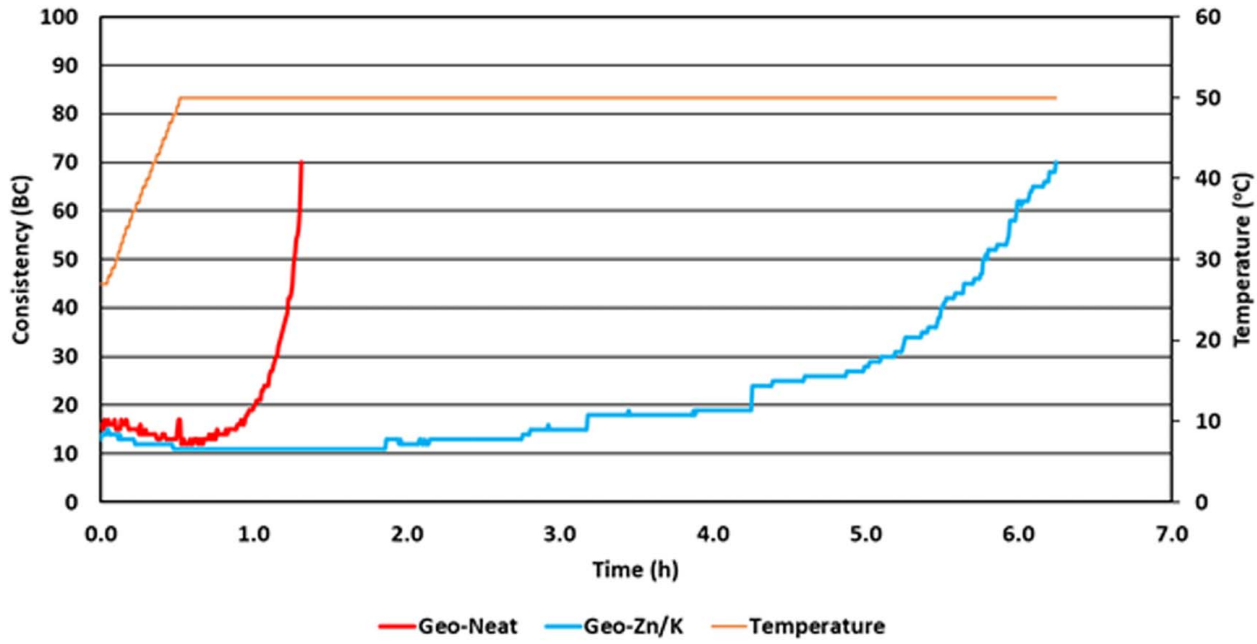

Fig. 4 Workability and gelation time at BHCT of 50 °C and pressure of 14 MPa

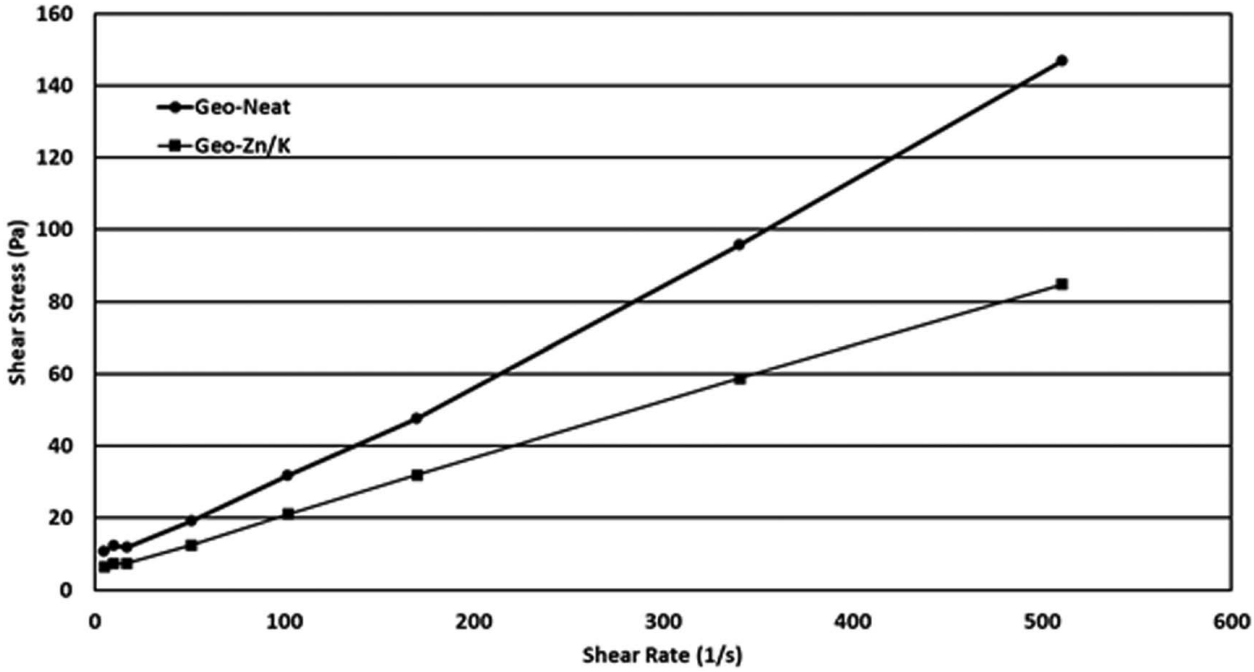

Fig. 5 Viscosity profile at 50 °C BHCT

metal bolts; the setup is presented in Fig. 3. Samples were conditioned prior of placement in the setup and cured for 7 days at BHST of 70 °C and pressure of 14 MPa. The test setup was designed to pump water from the bottom, using a linear gradual increase in pressure, where any water out would be detected by a flowmeter connected to the top outlet of the setup. After breaking sealability, the pressure and amount of water escaping the setup was recorded.

2.4 Composition and Structural Analysis

2.4.1 Phase Change. After curing samples, it is expected that there are multiple crystalline phase changes affected by temperature, pressure, and the chemical composition used. These changes were observed throughout the curing periods using a Bruker-AXS Micro-diffractometer D8 Advance, which uses a CuKα radiation (40.0 kV, 25.0 mA) with a 2θ range from 5 deg to 92 deg with 1 deg/min step and 0.010 deg increment. Samples collected from UCS tests were crushed and grounded into powder manually and drying was conducted at 40 °C in a vacuum oven for 24 h to avoid any solid–gas reaction and ensure the removal of water particles.

2.4.2 Microstructure Analysis. Scanning electron microscopy was conducted using a Gemini Supra 35VP (ZEISS) to examine microstructure post curing phase. Samples were retrieved from cured samples, cut into thin sections (thickness 1–2 mm), and emerged in epoxy to avoid any phase change or solid–gas, solid–solid reactions. The samples were smoothed and coated under vacuum with a palladium (Pd) layer of 10 nm prior to examination.

3 Results and Discussions

3.1 Workability and Gelation Time. The consistency profiles of geopolymer samples, both the neat and with chemical admixtures, are presented in Fig. 4. It was observed that the Geo-Neat had a workability period of approximately 1.2 h (h) (~73 min) and a gelation time of around 0.1 h (~6 min). On the other hand, the addition of Zn^{2+} and K^{+} species created a retarding effect making the workability reach around 5.5 h (~330 min) and a setting time of around 0.74 h (~44 min). It has been observed that the combination of Zn^{2+} and K^{+} has created a retarding effect in comparison with Geo-Neat sample by extending workability from ~1.22 h to ~5.5 h. Cavallotti et al. [31] showed that Zn^{2+} species

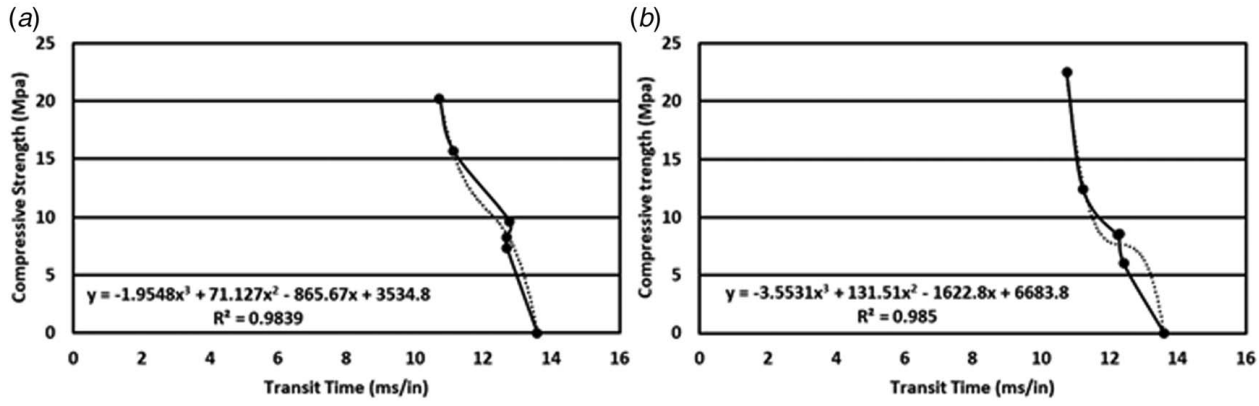

Fig. 6 Uniaxial compressive strength plotted versus the transit time for (*a*) Geo-Neat and (*b*) Geo-Zn/K

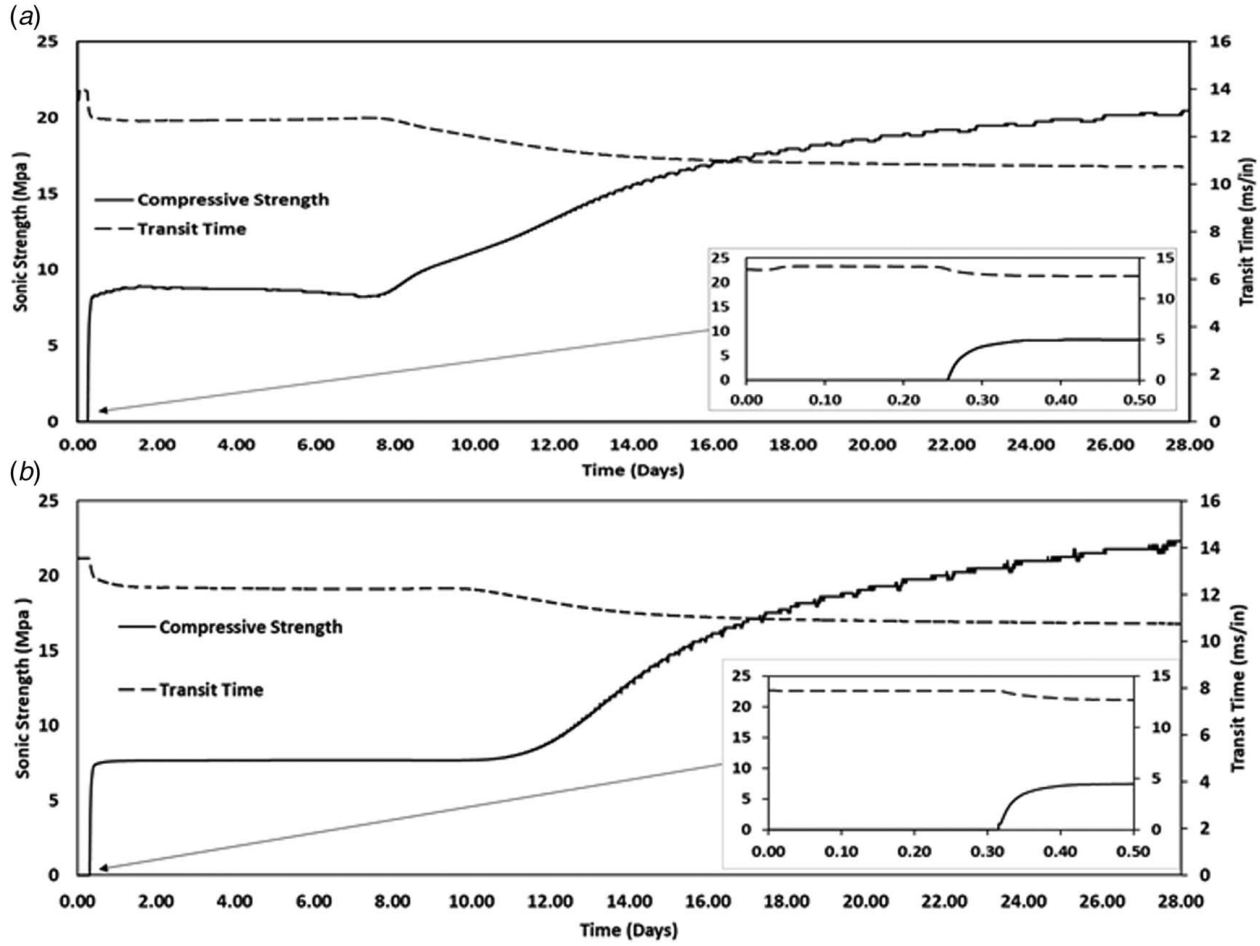

Fig. 7 UCA measurements for (*a*) Geo-Neat and (*b*) Geo-Zn/K

has a tendency to engage in hydroxylated alumina. In addition, it has the tendency to capture OH^- groups and produce zinc hydroxide (ZnO), which contributes to the poisoning effect. The current geopolymer system contains CaO by 9.94 wt% and high concentrations of OH^- which imply the possible formation of a Ca-Zn phase ($Ca(Zn(OH)_3)_2.2H_2O$). Such effects have been reported in previous studies of Zn effects in cement systems and alkali-activated systems [32,33]. Garg and White [34] investigated the effect of zinc oxide (ZnO) on high/low Ca alkali-activated system. They were able to correlate the effect of Zn^{2+} species on prolonging setting time of high Ca systems while not observing any significant effect on low calcium content systems. Their conclusion mainly focused on the

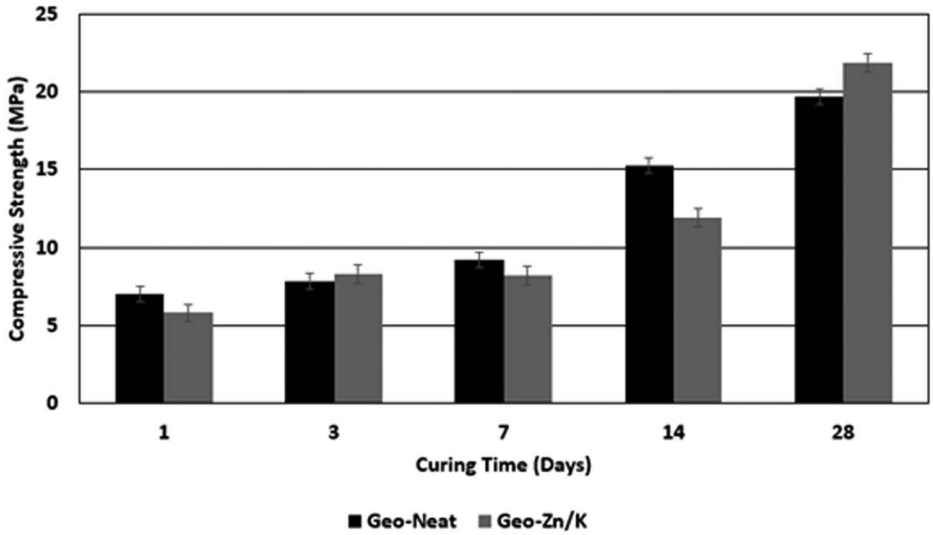

Fig. 8 Average UCS measurements of mix designs up to 28 days

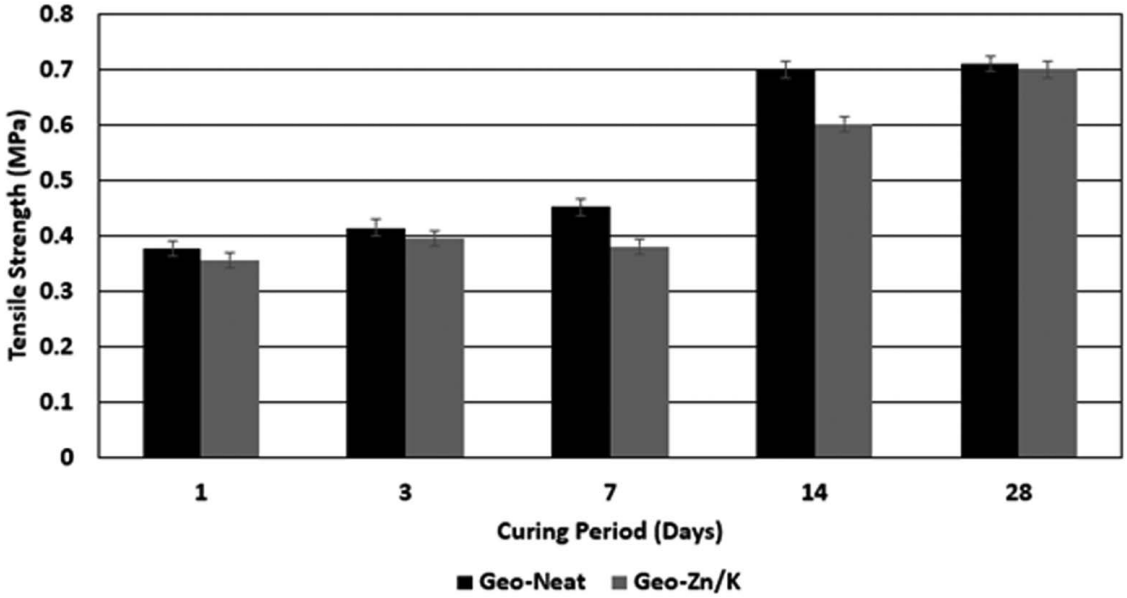

Fig. 9 Average tensile strength of mix designs

formation of Ca-Zn phases, which have the ability of poisoning C-(N)-A-S-H gel where Zn is incorporated homogenously through a "Ca depletion" mechanism where the development of Ca-Zn phases infects local undersaturated pore solutions which evidently leads to the retardation effect. In addition to the Zn's effect on Ca contained in the system, it has been found that incorporate with alkali activators, whether sodium (Na) or K-based systems, can also happen. A study by Wang et al. [35] indicates that Zn in geopolymer systems can inhibit alkali-activation reactions through the formation of metastable K/Na-Zn phases, which does not have any significant effect on primary products of N-(K)-A-S-H structure. This was concluded by investigating $Q^4(4Al)$ and $Q^4(3Al)$ through ^{29}Si MAS NMR spectra, which indicated the increase in number of $Q^4(4Al)$ sites leading to a decrease in the Si/Al ratio that point to the phenomena created by the partial replacement of Zn^{2+} for Na^+/K^+. N-(K)-A-S-H gels are intermediate products before the 3D network of geopolymers are completed [36]. However, in alkali-activated based systems, N-(K)-C-A-S-H phases are the final product. These observations support the retardation phenomena caused by Zn^{2+} ions.

3.2 Viscosity Profile. Geopolymer mix designs exhibit a non-Newtonian fluid behavior with the presence of yield stress as shown in Fig. 5. The shear stress of Geo-Neat was larger than the shear stress of the Geo-Zn/K slurry at the different evaluated shear

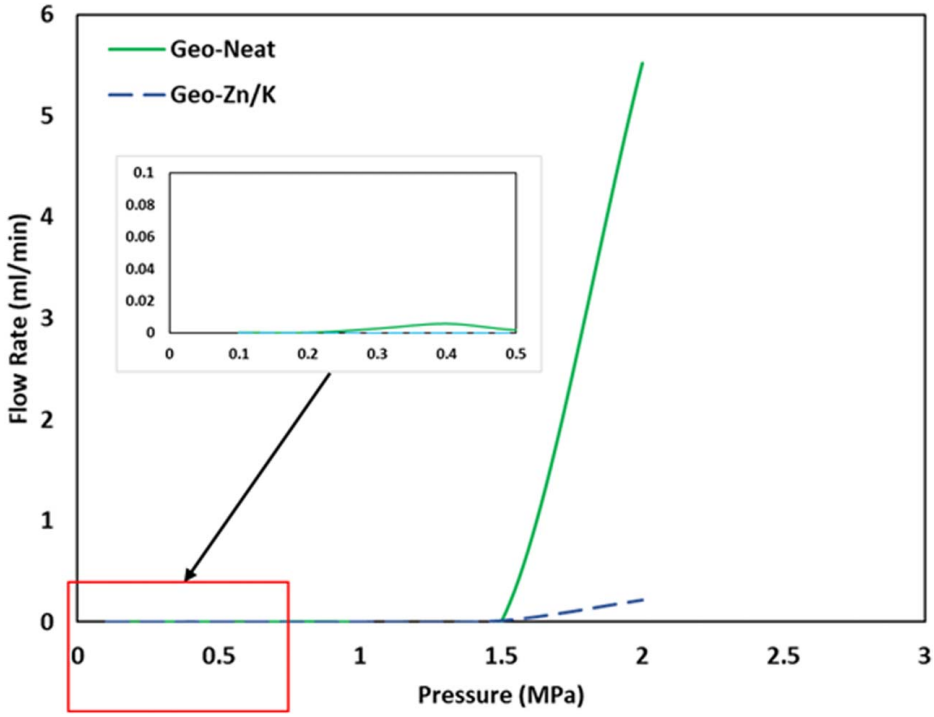

Fig. 10 Hydraulic sealability test results for clean steel casing

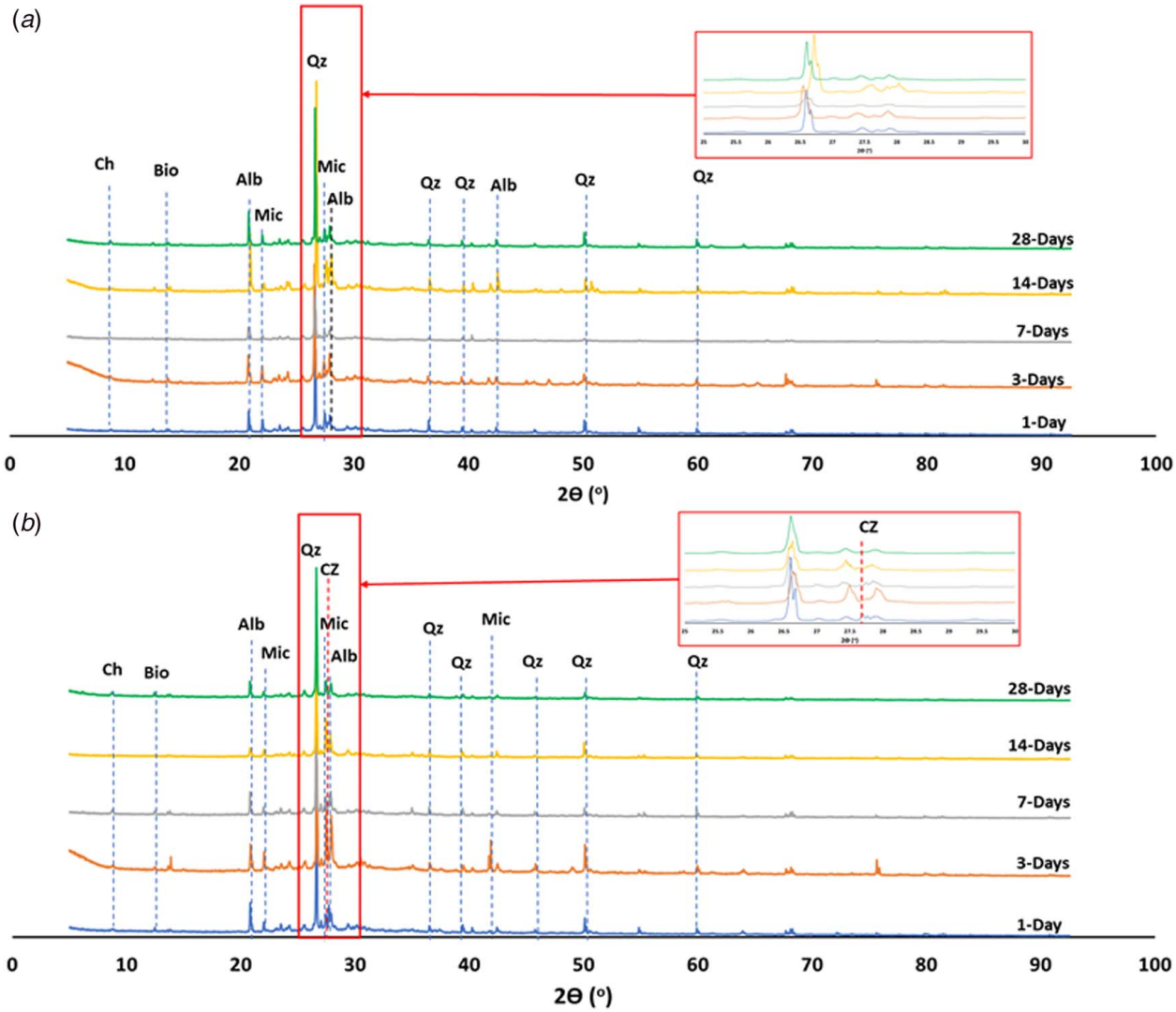

Fig. 11 XRD measurements of cured (*a*) Geo-Neat and (*b*) Geo-Zn/K up to 28 days

rates. By the addition of chemical admixtures, a reduction in viscosity can be observed for all the applied shear rates. Thus, it might be concluded that the chemical stability of the geopolymer colloidal system was affected by the addition of chemical admixtures.

3.3 Ultrasonic Cement Analyzer. The UCA was designed to measure sonic strength of OPC by detecting the travel time of ultrasound waves through the sample and applying a predetermined algorithm to estimate the sonic strength. Thus, a custom algorithm was developed by plotting the UCS data versus transit time. Afterward, the created algorithm was introduced to the UCA to convert the recorded transit time to sonic strength (see Fig. 6).

The sonic strength development for Geo-Neat and Geo-Zn/K was measured for a period of 28 days and under BHST conditions (70 °C and 14 MPa), presented in Fig. 7. It has been observed for Geo-Neat, the initial strength development starts after ~6 h from initial mixing ($t = 0$), stabilizing for around 7 days at around 8 MPa of compressive strength and then increase gradually to reach around 20 MPa after 28 days. On the other hand, Geo-Zn/K started to develop strength after ~7.5 h, maintaining a compressive strength of around 6 MPa for 11 days and then gradually increase to reach a compressive strength of around 21 MPa.

The effect of Zn^{2+} ions can be attributed to the similar poisoning phenomena mentioned in the *workability and gelation time* section, where Zn/K poisoning have occurred to the nucleation sites of N(K)-A-S-H gel of which the geopolymerization reaction was delayed due to the formation of Ca-Zn [35]. The differences surrounding the early strength development between Geo-Neat and Geo-Zn/K, ~1.5 h, indicates a delay in setting and hardening process.

3.4 Uniaxial Compressive Strength. The average compressive strength of mix designs for a period up to 28 days is shown in Fig. 8. It was observed that the compressive strength, elasticity, and tensile strength are interlinked properties where the increase elasticity of cementitious material can contribute in decreasing the

Table 3 Mineral composition extracted from XRD patterns of cured mix designs up to 28 days

Mineral	Chemical composition
Quartz	SiO_2
Albite	$NaAlSi_3O_8$
Microcline	$KAlSi_3O_8$
Chamosite	$(Fe^{2+},Mg,Al,Fe^{3+})_6(Si,Al)_4O_{10}(OH,O)_8$
Biotite	$K(Mg,Fe)_3(AlSi_3O_{10})(F,OH)_2$
Calcium Zinc Silicate	$CaZnSi_3O_8$

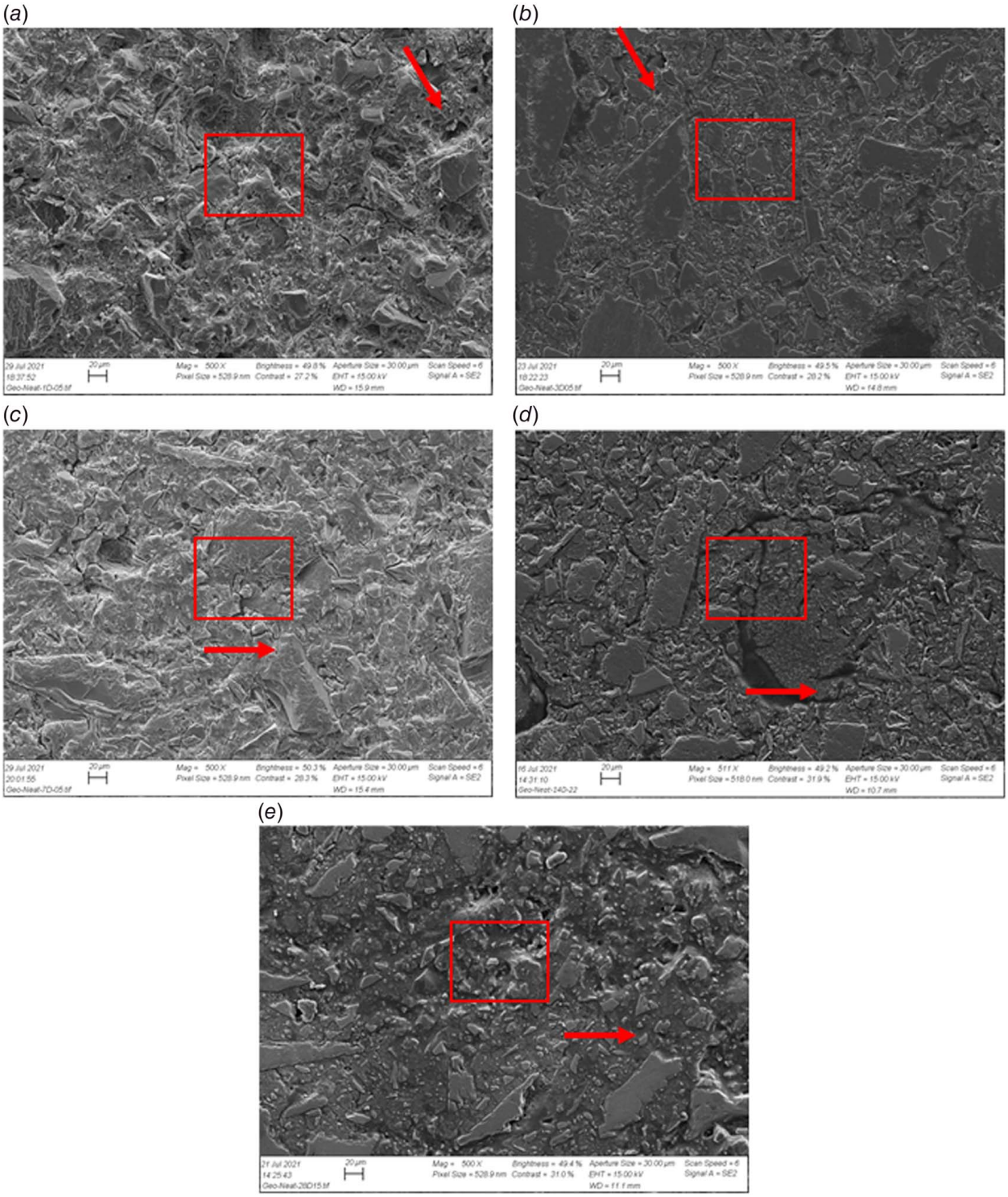

Fig. 12 SEM images (range of 20 μm) of Geo-Neat at (*a*) 1 day, (*b*) 3 days, (c) 7 days, (*d*) 14 days, and (e) 28 days; red square highlighting the focus area; red arrow for unreacted particles

compressive and tensile strength properties required to maintain zonal isolation [37]. This behavior is instinct of all cementitious materials unless reinforcements are used in the structure of the material. The results show that the compressive strength of Geo-Neat gradually increased throughout the curing period while maintaining a close compressive strength of around 8 to 9 MPa during the first 7 days reaching to ~20 MPa after 28 days. On the other hand, the compressive strength of Geo-Zn/K was following an increasing trend, similar to Geo-Neat's trend, starting from around ~6 MPa after 1 d to reach around 21 MPa after 28 days. It is evident from the results presented in Fig. 8 that the addition of Zn^{2+} and K^{+} species have reduced the compressive strength development of geopolymer samples in the early stages up to 14 days. The presence of Zn^{2+} species has a poisoning effect on geopolymer systems as discussed previously. In the presented chemical system, it is believed that the Zn^{2+} species have negatively affected the development of 3D networks by inhibiting the formation of geopolymer gels and slowing the condensation process [38]. Many researchers have examined the influence of increasing the weight of Zn^{2+} species (≤10 wt%) to improve the compressive strength

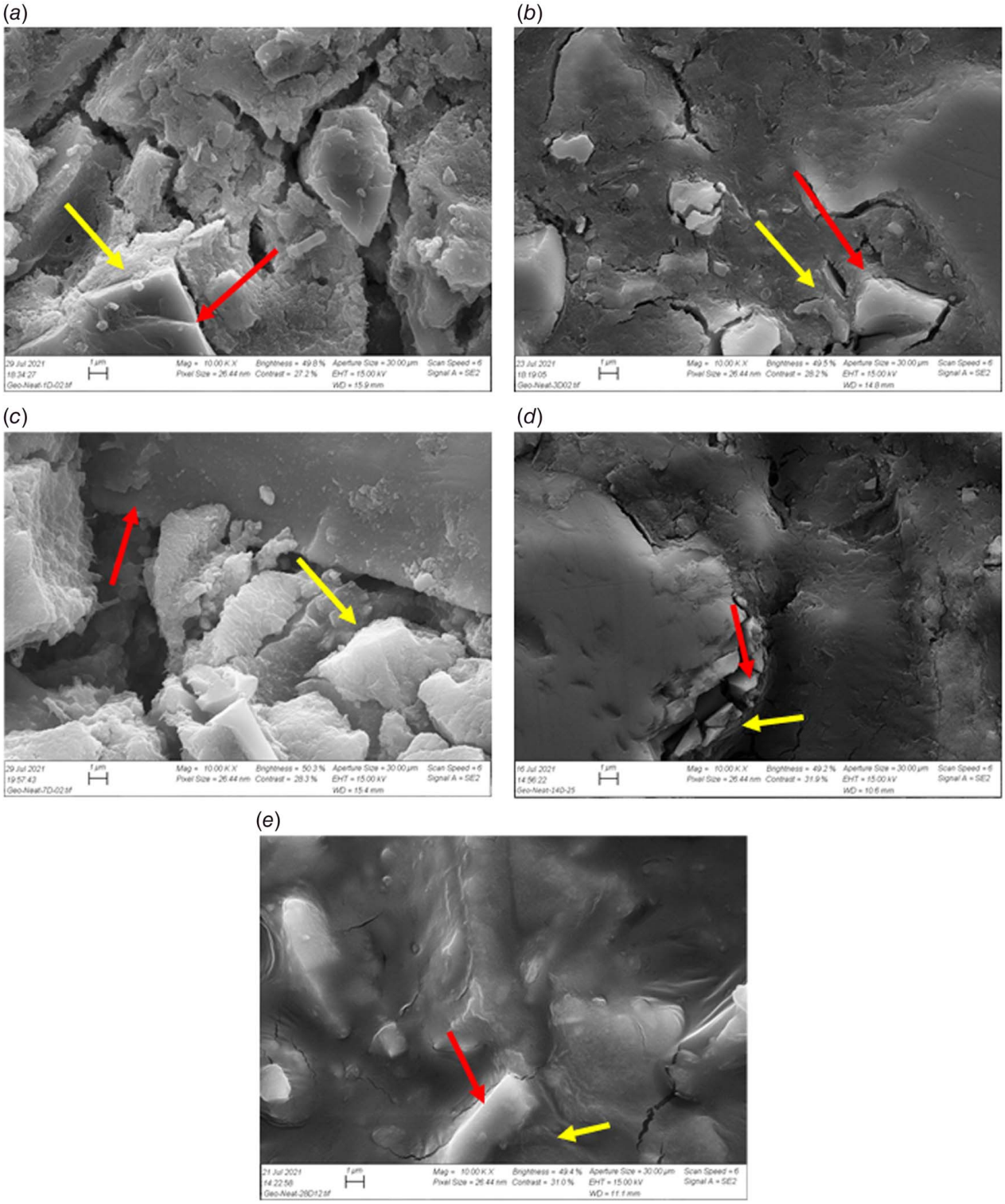

Fig. 13 SEM images (range of 1 μm) of Geo-Neat at (*a*) 1 day, (*b*) 3 days, (c) 7 days, (*d*) 14 days, and (e) 28 days; red arrow for unreacted particles and yellow arrow for binder formation

of geopolymer systems [38,39]; while this can be an interesting point to improve the compressive strength of the mix design discussed in the study, the effect on slurry properties, specifically workability, should be taken into account.

3.5 Indirect Tensile Test (Brazilian Test). The tensile strength measurements for mix designs are presented in Fig. 9. It has been observed that both mix designs had a relatively increasing tensile strength starting from ~0.38 MPa reaching to around ~0.7 MPa. Although no clear indication of how the addition of Zn^{2+} and K^{+} species may affect the tensile strength in long-term periods, it may be pointed out the trend seen by Geo-Zn/K at early stages of which shows a delay in the strength development. The reality of downhole conditions can exert force on different directions to the cement sheath, jeopardize the integrity of the

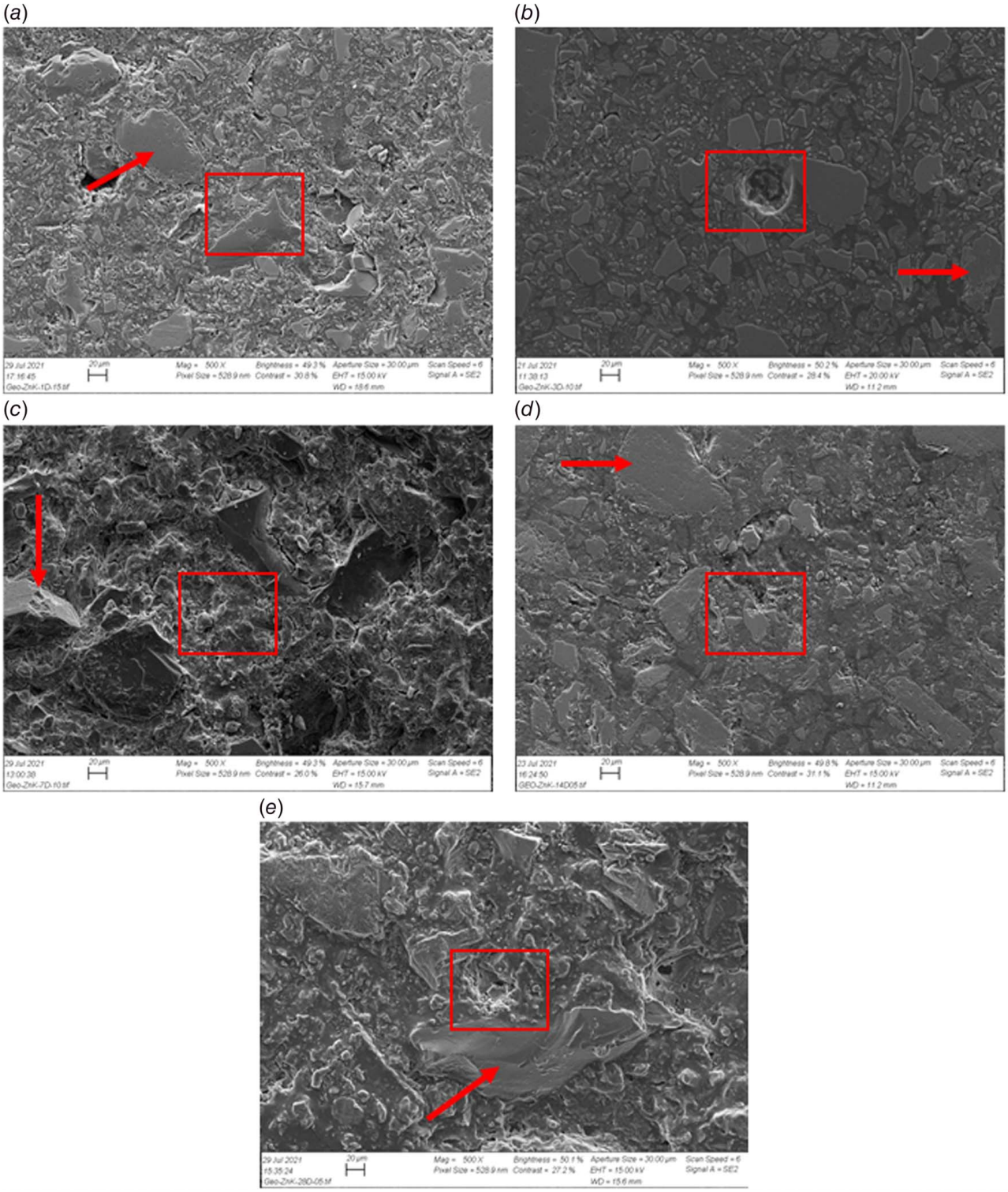

Fig. 14 SEM images (range of 20 μm) of Geo-Zn/K at (*a*) 1 day, (*b*) 3 days, (c) 7 days, (*d*) 14 days, and (e) 28 days; red square highlighting the focus area; red arrow for unreacted particles

cementitious material, and eventually the integrity of production operations. The forces applied over the cement sheath may lead to having low tensile strength or debonding/poor bonding of cementitious material to casing [40]. The effect of Zn^{2+} and K^{+} species on the tensile strength throughout the curing periods can be linked as well to the poisoning effect of Zn^{2+} species, which was highlighted in Sec. 3.4. The effect of chemical admixtures specifically Zn^{2+} species seems to be highly significant when it comes to mechanical properties development.

3.6 Hydraulic Sealability. The test was conducted to examine the material's ability to maintain sealability at the interface of barrier material and casing systems to ensure that the admixtures

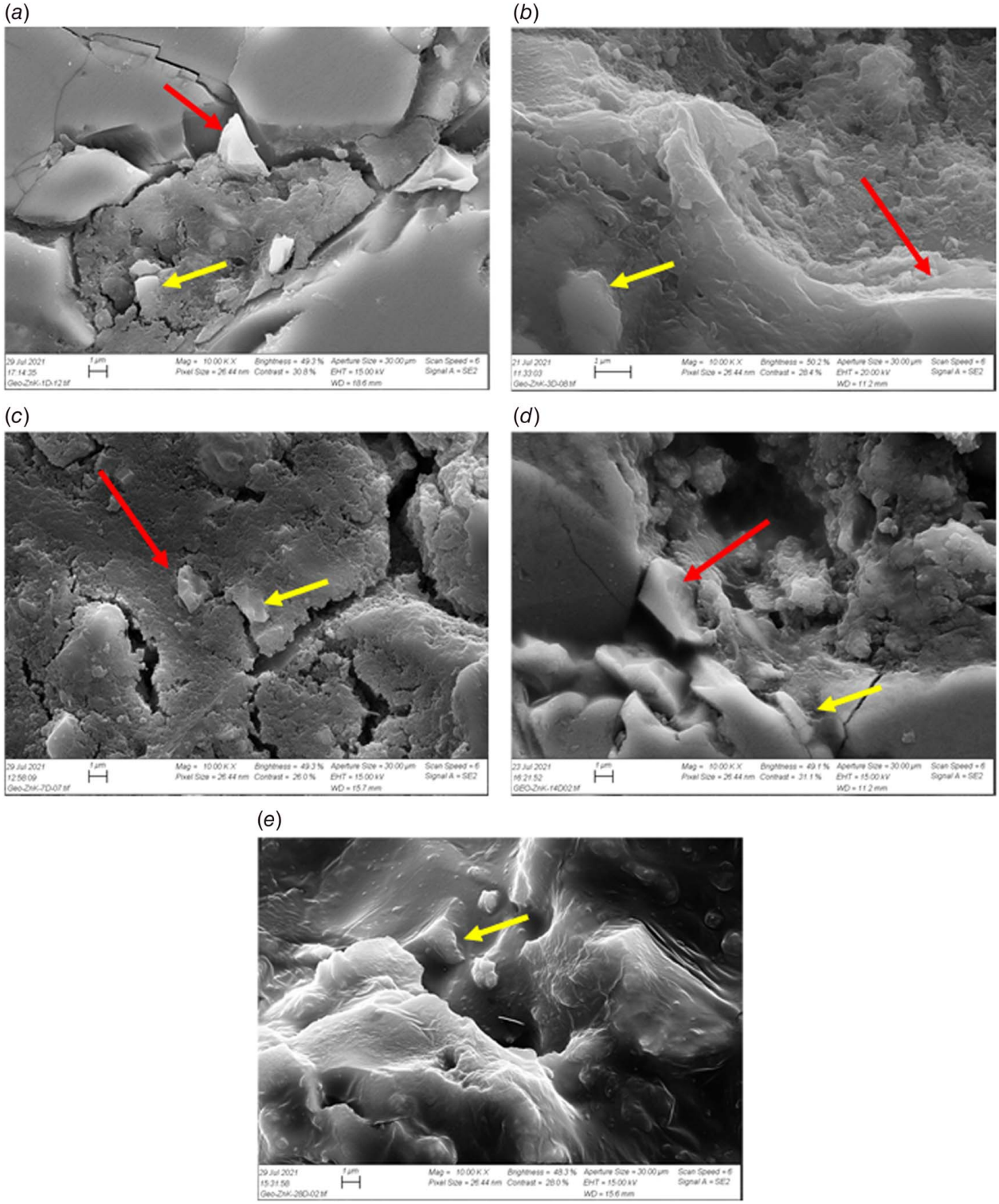

Fig. 15 SEM images (range of 1 μm) of Geo-Zn/K at (*a*) 1 day, (*b*) 3 days, (c) 7 days, (*d*) 14 days, and (e) 28 days; red arrow for unreacted particle and yellow arrow for binder formation

do not impact the main function of the barrier. The results of hydraulic sealability examination are presented in Fig. 10, where the water flowrate (ml/min) is presented versus the pressure (bar). For Geo-Neat, it has been observed that the hydraulic sealability has been compromised at a pressure of around ~0.3 MPa. Some minor fluctuations have been observed and may be attributed to the differential pressure between the water pump and the pressure already existing inside the hydraulic sealability test. On the other hand, Geo-Zn/K failed hydraulic integrity at ~1.5 MPa where the initial flowrate indications were recorded. These observations indicate a significant effect of using Zn^{2+} and K^{+} species as chemical admixtures on the material's ability to resist leakage. The higher sealability exhibited by Geo-Zn/K mix design can be attributed to the effect of Zn^{2+} species on the geopolymer system under study. The use of Zn has been recognized previously by Carter et al. [41] to be an effective additive in the expansion of cement, due to the gas forming

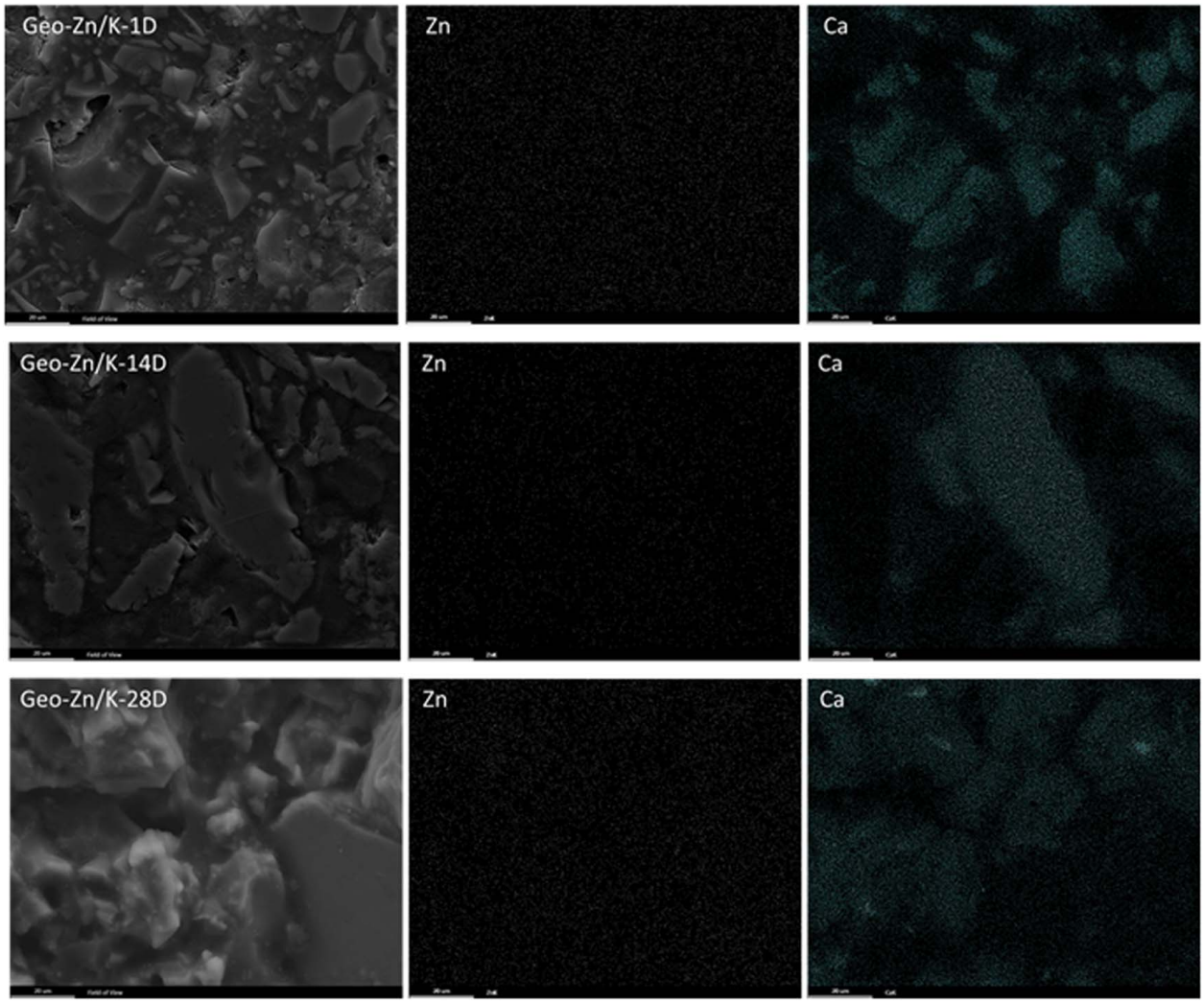

Fig. 16 SEM mapping imagery of Zn and Ca for Geo-Zn/K 1, 14, and 28 days

mechanism, which Zn eases in cementitious systems. Gas forming expansion happens due to the interaction between additive species, in this study Zn^{2+} species, and the alkali molecules in the cementitious medium where relatively small hydrogen gas bubbles are formed. The reaction occurs in the presence of Al particles, which are available in abundance in the system under study. Correlating to Carter et al. [41] conclusions, it seems that the conditions of this chemical reaction whether they are temperature, pressure, or chemical system were in favor for an expansion mechanism to be triggered by the presence of Zn^{2+} species. It should be noted that further consideration of this expansion phenomena should be examined considering the kinetics of the reaction and identifying the role of K^{+} species, which was not highlighted during this study due to the very little amount used in the chemical system presented.

3.7 Phase Change. X-Ray diffraction (XRD) patterns of the cured samples of Geo-Neat and Geo-Zn/K are presented in Figs. 11(*a*) and 11(*b*). The main phase recorded in both patterns was Quartz (Qz) with the presence of minor phases of albite (Alb), microcline (Mic), chamosite (Ch), biotite (Bio) and minor presence of calcium zinc silicate (CZ) peak in Geo-Zn/K samples. The composition of the mentioned minerals is presented in Table 3. Similar trends have been observed throughout the XRD patterns of both cured mix designs, where Qz was constantly decreasing in peak intensity indicating the consumption of Si by the geopolymer binder. The presence of Alb and Mic peaks in K-activated system favors the formation of zeolite phases which can explain the crystalline pattern obtained from the XRD results [17]. Thus, the increase in mechanical properties (e.g., compressive and tensile strengths) can be attributed to the formation of these zeolite phases. A study by Prud'homme et al. [42] investigated the effect of raw material and Si properties on the formation of zeolite phases in geopolymer material. It was determined that the properties of raw material and type of activator play a major role in the formation of zeolite phase. It can be concluded that in this geopolymer system properties of raw material may have favored the formation of a crystalline phase, mainly composed of zeolite, considering the enhancement of mechanical properties observed throughout the curing period. The effect of Zn^{2+} species was observed by detecting calcium zinc silicate (CZ) phase at peak 27.8 deg where the peak was minor in comparison to other existing peaks such as microcline and albite. The minor presence of such peaks can be attributed to the limited amount of Zn^{2+} species (0.3 wt%) used in the mix design (Table 2). In previous studies, Zn was detected mainly in the form of zinc oxide (ZnO), but that was highly dependent on the type of Zn used [34,35]. Although a CZ peak is present, it is still not a definite indication of the form/structure of the mineral formed and would require much thorough characterization to clearly identify the type of Ca-Zn phases formed with in Geo-Zn/K mix designs.

3.8 Microstructure Analysis. The scanning electronic microscopic (SEM) images of samples cured for a period up to 28 days

are presented in Figs. 12 and 13 for Geo-Neat and in Figs. 14 and 15 for Geo-Zn/K. It must be noted that the samples were collected through cutting from cured mold samples prepared for UCS tests to minimize any cracks caused by mechanical forces. The images present areas in the range of 20 μm presented for each curing period of every sample. The areas of focus and interest were marked with the red box (Figs. 12 and 14). The SEM images show significant change in microstructure between early curing periods (up to 7 days) and long curing periods (up 28 days). The visualization of unreacted aluminosilicate particles aligns with previous studies, where the presence of these unreacted particles was confirmed by having a plate-shaped structure around empty areas [43–45]. Throughout the SEM images, it can be noticed that a more homogeneous structure was formed as the curing time progresses which explains the increase in mechanical properties of the samples. The effect of Zn^{2+} species and K^{+} species was not detected in the SEM images where this may be attributed to the low amount of chemical admixtures used in Geo-Zn/K. The identification of these phenomena will require more advanced techniques to compensate the current angular resolution from the XRD.

Mapping imagery in Fig. 16 shows a homogeneous distribution of Zn and Ca throughout Geo-Zn/K samples. The distribution of these elements was overlapping, though with much less concentration of Zn, which gives the presumption of chemical interactions occurring between these two elements. The formation of Ca-Zn phases cannot be verified from these imageries but raises the question of how these elements are interacting, what type of chemical structures are present, and what retardation mechanism is truly occurring throughout the chemical system and its poisoning effects during the curing period. To tackle these questions, advanced techniques such as solid Mass-NMR must be applied, especially due to the low amount of chemical admixtures introduced to this geopolymer chemical system.

4 Conclusion

Rock-based geopolymer systems with Zn^{2+} and K^{+} species as retarding agents were examined under downhole conditions using a testing matrix developed to initially test material on a lab-scale under field conditions. Retardation was achieved by using Zn^{2+} species while the effect of K^{+} species was not observed clearly due to the little amount introduced in the system. The chemical admixtures reduced the viscosity profile of the investigated slurry. Through the examination of mechanical properties, a delay in early strength development has been observed up to until 14 days due to a poisoning phenomenon, which was anticipated to be a result of the development of Ca-Zn phases that hurdles the nucleation and formation of geopolymeric structure. Composition analysis combined with SEM images showed the development of new crystalline phases and an ongoing reaction slowly incorporating particles into the binder structure throughout the curing period. More thorough characterization techniques are required to validate the presence of Ca-Zn phases and point out any other poisoning phases that might have developed throughout the reaction. The development of chemical admixtures for geopolymer systems opens the door to more tailored solutions that can fit with the assigned bottomhole conditions to ensure a systematic synergy between slurry, mechanical, and structural properties which can ease any future application of the material.

Acknowledgment

The authors gratefully acknowledge TOTAL Norge, AkerBP, ConocoPhillips, and Research Council of Norway for financially supporting the SafeRock KPN Project (RCN #319014) at the University of Stavanger, Norway. Special thanks to Laurent Delabroy, Johan Kverneland, Roy Gordon Middleton, Ivar Blaauw, Carl Johnson, and Gunnar Lende for their technical inputs. The authors would also like to thank Adijat Ayobami Ogienagbon for her assistance in the hydraulic sealability experiments, Caroline Ruud for her help in composition analysis, and Pedram Gargari for his assistance in experimental work.

Funding Data

This study was funded by Research Council of Norway (KD) through the Department of Energy and Petroleum Engineering (IEP), University of Stavanger (UiS).

Conflict of Interest

There are no conflicts of interest.

References

[1] Pacheco-Torgal, F., Labrincha, J., Leonelli, C., Palomo, A., and Chindaprasit, P., 2014, *Handbook of Alkali-Activated Cements, Mortars and Concretes*, Elsevier, New York.

[2] Provis, J. L., Fernández-Jiménez, A., Kamseu, E., Leonelli, C., and Palomo, A., 2014, "Binder Chemistry—Low-Calcium Alkali-Activated Materials," *Alkali Activated Materials: State-of-the-Art Report, RILEM TC 224-AAM*, J. L. Provis, and J. S. J. van Deventer, eds., Springer Netherlands, Dordrecht, pp. 93–123.

[3] Duxson, P., Fernández-Jiménez, A., Provis, J. L., Lukey, G. C., Palomo, A., and van Deventer, J. S. J., 2007, "Geopolymer Technology: The Current State of the Art," J. Mater. Sci., **42**(9), pp. 2917–2933.

[4] Bernal, S. A., Provis, J.L., and Fernandez-Jamenez, A., 2014, *Alkali Activated Materials: State-of-the-Art Report, RILEM TC 224-AAM*, J. L. Provis, and J. S. J. van Deventer, eds., Springer Netherlands, Dordrecht, pp. 59–91.

[5] Davidovits, J., 2005, Geopolymer, Green Chemistry and Sustainable Development Solutions: Proceedings of the World Congress Geopolymer 2005, Geopolymer Institute.

[6] Davidovits, J., 2015, *Geopolymer Chemistry and Applications*, 4th ed., Geopolymer Institute, France.

[7] Davidovits, J., 1994, "Properties of Geopolymer Cements," First International Conference on Alkaline Cements and Concretes, Ukraine, pp. 131–149.

[8] Davidovits, J., 1991, "Geopolymers: Inorganic Polymeric New Materials," J. Therm. Anal. Calorim., **37**(8), pp. 1633–1656.

[9] Davidovits, J., 1987, "Ancient and Modern Concretes: What is the Real Difference," Concr. Int., **9**(12), pp. 12–23.

[10] Davidovits, J., 1994, "Global Warming Impact on the Cement and Aggregates Industries," World Resour. Rev., **6**(2), pp. 263–278.

[11] Khalifeh, M., 2016, "Materials for Optimized P&A Performance: Potential Utilization of Geopolymers," Ph.D. Thesis, http://hdl.handle.net/11250/2396282.

[12] Khalifeh, M., Hodne, H., Saasen, A., Integrity, O., and Eduok, E. I., 2016, "Usability of Geopolymers for Oil Well Cementing Applications: Reaction Mechanisms, Pumpability, and Properties," The SPE Asia Pacific Oil & Gas Conference and Exhibition, Perth, Australia.

[13] Khalifeh, M., Motra, H. B., Saasen, A., and Hodne, H., 2018, "Potential Utilization for a Rock-Based Geopolymer in Oil Well Cementing," International Conference on Offshore Mechanics and Arctic Engineering, Madrid, Spain, American Society of Mechanical Engineers, vol. 51296, p. V008T11A037.

[14] Khalifeh, M., Saasen, A., Hodne, H., Godøy, R., and Vrålstad, T., 2018, "Geopolymers as an Alternative for Oil Well Cementing Applications: A Review of Advantages and Concerns," ASME J. Energy Resour. Technol., **140**(9), p. 092801.

[15] Khalifeh, M., Saasen, A., Hodne, H., and Motra, H. B., 2019, "Laboratory Evaluation of Rock-Based Geopolymers for Zonal Isolation and Permanent P&A Applications," J. Pet. Sci. Eng., **175**, pp. 352–362.

[16] Khalifeh, M., Saasen, A., Vralstad, T., and Hodne, H., 2014, "Potential Utilization of Class C Fly Ash-Based Geopolymer in Oil Well Cementing Operations," Cem. Concr. Compos., **53**, pp. 10–17.

[17] Khalifeh, M., Saasen, A., Vrålstad, T., Larsen, H. B., and Hodne, H., 2016, "Experimental Study on the Synthesis and Characterization of Aplite Rock-Based Geopolymers," J. Sustainable Cem.-Based Mater., **5**(4), pp. 233–246.

[18] Salehi, S., Khattak, M. J., Ali, N., Ezeakacha, C., and Saleh, F. K., 2018, "Study and Use of Geopolymer Mixtures for Oil and Gas Well Cementing Applications," ASME J. Energy Resour. Technol., **140**(1), p. 012908.

[19] Salehi, S., Khattak, M. J., Rizvi, H., Karbalaei, S., and Kiran, R., 2017, "Sensitivity Analysis of Fly Ash Geopolymer Cement Slurries: Implications for Oil and Gas Wells Cementing Applications," J. Nat. Gas Sci. Eng., **37**, pp. 116–125.

[20] Salehi, S., Ali, N., Khattak, M., and Rizvi, H., 2016, "Geopolymer Composites," SPE Annual Technical Conference and Exhibition, Dubai, UAE, Society of Petroleum Engineers.

[21] Chen, L., Wang, H., Xin, J., Wu, X., Wang, W., Zhao, H., Kong, L., and Xu, C., 2011, "Research on Techno-Economic Performance of the Geopolymeric Cement With Oil Shale Residue and Slag," New Build. Mater., **3**.

[22] Mobili, A., Belli, A., Giosuè, C., Bellezze, T., and Tittarelli, F., 2016, "Metakaolin and Fly Ash Alkali-Activated Mortars Compared With Cementitious Mortars at the Same Strength Class," Cem. Concr. Res., **88**, pp. 198–210.
[23] Alex, T. C., Kalinkin, A. M., Nath, S. K., Gurevich, B. I., Kalinkina, E. V., Tyukavkina, V. V., and Kumar, S., 2013, "Utilization of Zinc Slag Through Geopolymerization: Influence of Milling Atmosphere," Int. J. Miner. Process., **123**, pp. 102–107.
[24] Nath, S. K., 2020, "Fly ash and Zinc Slag Blended Geopolymer: Immobilization of Hazardous Materials and Development of Paving Blocks," J. Hazard. Mater., **387**, p. 121673.
[25] Duxson, P., Provis, J., Lukey, G., Van Deventer, J., Separovic, F., and Gan, Z., 2006, "39K NMR of Free Potassium in Geopolymers," Ind. Eng. Chem. Res., **45**(26), pp. 9208–9210.
[26] Lizcano, M., Kim, H. S., Basu, S., and Radovic, M., 2012, "Mechanical Properties of Sodium and Potassium Activated Metakaolin-Based Geopolymers," J. Mater. Sci., **47**(6), pp. 2607–2616.
[27] Chamssine, F., Khalifeh, M., Eid, E., Minde, M. W., and Saasen, A., 2021, "Effects of Temperature and Chemical Admixtures on the Properties of Rock-Based Geopolymers Designed for Zonal Isolation and Well Abandonment," ASME 2021 40th International Conference on Ocean, Offshore and Arctic Engineering, Online Conference, vol. 10, Petroleum Technology, p. V010T11A031.
[28] American Petroluem Institute, 2013, API RP 10B-2, 2nd ed., Recommended Practice for Testing Well Cements.
[29] American Petroluem Institute, 2017, API TR 10TR7, 1st ed., Mechanical Behavior of Cement.
[30] American Society for Testing and Materials, 2016, ASTM D-3967-16, Standard Testing Method for Splotting Tensile Strength of Intact Rock Core Specimens.
[31] Cavallotti, R., Goniakowski, J., Lazzari, R., Jupille, J., Koltsov, A., and Loison, D., 2014, "Role of Surface Hydroxyl Groups on Zinc Adsorption Characteristics on α-Al2O3(0001) Surfaces: First-Principles Study," J. Phys. Chem. C, **118**(25), pp. 13578–13589.
[32] Tommaseo, C., and Kersten, M., 2002, "Aqueous Solubility Diagrams for Cementitious Waste Stabilization Systems. 3. Mechanism of Zinc Immobilizaton by Calcium Silicate Hydrate," Environ. Sci. Technol., **36**(13), pp. 2919–2925.
[33] Yousuf, M., Mollah, A., Hess, T. R., Tsai, Y.-N., and Cocke, D. L., 1993, "An FTIR and XPS Investigations of the Effects of Carbonation on the Solidification/Stabilization of Cement Based Systems-Portland Type V With Zinc," Cem. Concr. Res., **23**(4), pp. 773–784.
[34] Garg, N., and White, C. E., 2017, "Mechanism of Zinc Oxide Retardation in Alkali-Activated Materials: An in Situ X-Ray Pair Distribution Function Investigation," J. Mater. Chem. A, **5**(23), pp. 11794–11804.
[35] Wang, L., Geddes, D. A., Walkley, B., Provis, J. L., Mechtcherine, V., and Tsang, D. C., 2020, "The Role of Zinc in Metakaolin-Based Geopolymers," Cem. Concr. Res., **136**, p. 106194.
[36] Yang, J., Li, D., and Fang, Y., 2017, "Synthesis of Nanoscale CaO-Al_2O_3-SiO_2-H_2O and Na_2O-Al_2O_3-SiO_2-H_2O Using the Hydrothermal Method and Their Characterization," Materials, **10**(7), p. 695. https://www.mdpi.com/1996-1944/10/7/695
[37] Jafariesfad, N., Geiker, M. R., Gong, Y., Skalle, P., Zhang, Z., and He, J., 2017, "Cement Sheath Modification Using Nanomaterials for Long-Term Zonal Isolation of Oil Wells: Review," J. Pet. Sci. Eng., **156**, pp. 662–672.
[38] Zailan, S. N., Bouaissi, A., Mahmed, N., and Abdullah, M. M. A. B., 2020, "Influence of ZnO Nanoparticles on Mechanical Properties and Photocatalytic Activity of Self-Cleaning ZnO-Based Geopolymer Paste," J. Inorg. Organomet. Polym. Mater., **30**(6), pp. 2007–2016.
[39] Zidi, Z., Ltifi, M., Ayadi, Z. B., Mir, L. E., and Nóvoa, X., 2020, "Effect of Nano-ZnO on Mechanical and Thermal Properties of Geopolymer," J. Asian Ceram. Soc., **8**(1), pp. 1–9.
[40] Kamali, M., Khalifeh, M., Saasen, A., Godøy, R., and Delabroy, L., 2021, "Alternative Setting Materials for Primary Cementing and Zonal Isolation—Laboratory Evaluation of Rheological and Mechanical Properties," J. Pet. Sci. Eng., **201**, p. 108455.
[41] Carter, L., Waggoner, H., and George, C., 1966, "Expanding Cements for Primary Cementing," J. Pet. Technol., **18**(5), pp. 551–558.
[42] Prud'homme, E., Michaud, P., Joussein, E., and Rossignol, S., 2012, "Influence of Raw Materials and Potassium and Silicon Concentrations on the Formation of a Zeolite Phase in a Geopolymer Network During Thermal Treatment," J. Non-Cryst. Solids, **358**(16), pp. 1908–1916.
[43] Duxson, P., Provis, J. L., Lukey, G. C., Mallicoat, S. W., Kriven, W. M., and van Deventer, J. S. J., 2005, "Understanding the Relationship Between Geopolymer Composition, Microstructure and Mechanical Properties," Colloids Surf. A, **269**(1), pp. 47–58.
[44] Duxson, P., Lukey, G., Separovic, F., and Van Deventer, J., 2005, "Effect of Alkali Cations on Aluminum Incorporation in Geopolymeric Gels," Ind. Eng. Chem. Res., **44**(4), pp. 832–839.
[45] Xu, H., and Van Deventer, J. S. J., 2002, "Microstructural Characterisation of Geopolymers Synthesised From Kaolinite/Stilbite Mixtures Using XRD, MAS-NMR, SEM/EDX, TEM/EDX, and HREM," Cem. Concr. Res., **32**(11), pp. 1705–1716.